Editors' Suggestion | Featured in Physics

Realization of the Einstein-Podolsky-Rosen Paradox Using Radial Position and Radial Momentum Variables

Lixiang Chen,[1,*] Tianlong Ma,[1] Xiaodong Qiu,[1] Dongkai Zhang,[1] Wuhong Zhang,[1] and Robert W. Boyd[2,3]
[1]*Department of Physics, Jiujiang Research Institute, and Collaborative Innovation Center for Optoelectronic Semiconductors and Efficient Devices, Xiamen University, Xiamen 361005, China*
[2]*Department of Physics, University of Ottawa, 25 Templeton Street, Ottawa, Ontario K1N 6N5, Canada*
[3]*Institute of Optics, University of Rochester, Rochester, New York 14627, USA*

(Received 30 April 2019; revised manuscript received 24 June 2019; published 8 August 2019)

As is well known, angular position and orbital angular momentum (OAM) of photons are a conjugate pair of variables that have been extensively explored for quantum information science and technology. In contrast, the radial degrees of freedom remain relatively unexplored. Here we exploit the radial variables, i.e., radial position and radial momentum, to demonstrate Einstein-Podolsky-Rosen correlations between down-converted photons. In our experiment, we prepare various annular apertures to define the radial positions and use eigenmode projection to measure the radial momenta. The resulting correlations are found to violate the Heisenberg-like uncertainty principle for independent particles, thus manifesting the entangled feature in the radial structure of two-photon wave functions. Our work suggests that, in parallel with angular position and OAM, the radial position and radial momentum can offer a new platform for a fundamental test of quantum mechanics and for novel application of quantum information.

DOI: 10.1103/PhysRevLett.123.060403

Quantum entanglement lies at the heart of quantum mechanics and quantum information science and technology [1]. The concept of entanglement can be traced back to the famous "EPR paradox" that originated from a gedanken experiment proposed by Einstein, Podolsky, and Rosen (EPR), who questioned the completeness of quantum mechanics [2]. In their gedanken experiment, two spatially separated particles could have both perfect correlations in position and momentum. However, such a scenario suggests that the position and the momentum of the unmeasured particle are simultaneous realities, which is obviously in violation of Heisenberg's uncertainty relation. Bohm cast the EPR paradox into a modified discrete version for two entangled spin-1/2 particles [3]. Then Bell formulated the Bell inequality to show that the EPR argument invoking local realism leads to algebraic predictions that are in contradiction to quantum mechanics [4]. Up to now, many experiments have been performed, in the context of Bell inequalities, to show nonlocal correlations and favor quantum mechanics, but they are generally limited to discrete state-space only [5–9]. Distinct from Bell inequalities, the demonstration of EPR violation could also signify the quantum entanglement for continuous variables [10]. Such a demonstration was theoretically and experimentally realized by using continuous variables of quadrature-phase amplitudes for squeezed-light fields in nondegenerate parametric oscillators [11,12]. Also, the violation of the EPR criterion was observed by using the momentum-position entangled photon pairs produced by spontaneous parametric down-conversion (SPDC) [13]. Other experimental efforts ensued to exploit other continuous properties of photons, e.g., the transverse spatial modes of bright laser beams and entangled images from four-wave mixing [14,15]. Moreover, by imaging both the near- and far-field correlations, the full-field spatial entanglement was manifested [16,17].

Recent years have also witnessed a growing interest in the connection of structured photons with quantum entanglement [18]. The most typical example of structured photons are twisted photons that carry orbital angular momentum (OAM), whose high-dimensional features offer a new playground for quantum information applications [19–21]. In many applications, the natural candidate of choice to describe such twisted photons is the Laguerre-Gaussian (LG) modes [22]. The LG mode has a helical phase structure of $\exp(i\ell\phi)$, and each photon carries a well-defined OAM of $\ell\hbar$. In quantum optics, it is described by the eigenfunction of the OAM operator, $\hat{L}_z|\ell, p\rangle = \ell\hbar|\ell, p\rangle$, where $\hat{L}_z = i\hbar\partial/\partial\phi$. Analogously to the uncertainty principle in linear position and momentum, angular position and OAM also forms a pair of conjugate variables, which can be linked by a discrete Fourier relationship [23]. The discrete values of OAM result from the 2π periodic nature of the angle variable, in contrast to the continuous property for both linear position and momentum. It has been well established that photon pairs generated by SPDC exhibit high-dimensional OAM entanglement [24]. Also, the strong EPR correlations have been experimentally demonstrated for the azimuthal degrees of freedom of angular position and OAM, suggesting that both variables

are suitable for applications in quantum information processing [25]. However, OAM is related only to the azimuthal degree of freedom (d.o.f.) of a single photon. In contrast, the consequence of the radial d.o.f. of single photons still remained relatively unexplored. In some early efforts, the radial index p of LG modes was isolated from the azimuthal index ℓ to show its quantum content [26–28] via the Hong-Ou-Mandel interference or violation of a Bell inequality [29,30]. Akin to sorting the azimuthal OAM number [31,32], the elegant yet efficient schemes were devised to sort single photons according to individual radial index [33,34] or both radial and azimuthal indices [35], promisingly increasing the single photon's bandwidth for information encoding [36,37]. However, we note that the EPR paradox has not yet been demonstrated using the radial degrees of freedom of quantum particles. While the discrete OAM number is related to the periodic nature of angular position, the discrete radial index cannot be mathematically derived from the semi-infinite half-space nature of the radial position. Besides, a canonical operator for the radial index has been formally constructed [27,28], which, however, appears as the differential forms of both angle and radial variables and obviously cannot satisfy the fundamental commutation relation with the radial position. Therefore, a major incentive for the present work is to formulate and demonstrate EPR correlations using the semi-infinite radial position and its conjugate variable of continuous radial momentum. Our theoretical and experimental results suggests that, in addition to angular position and OAM, these two radial variables can add to the optical tool box for a fundamental test of quantum mechanics and novel application of quantum information.

In our scheme, we employ the spatially entangled photon pairs generated by SPDC to test the radial version of EPR paradox. In the process of SPDC with a fundamental Gaussian pump beam, a pump photon is down-converted at one particular transverse position into a pair of photons, say signal (A) and idler (B), while conserving energy and momentum. Because of their common birthplace, the generated photons are well correlated in vector position, namely, $\mathbf{r}_A = \mathbf{r}_B$. Consequently, their radial positions should also be highly correlated, i.e., $r_A = r_B$, where $r_A = |\mathbf{r}_A|$ and $r_B = |\mathbf{r}_B|$, as is illustrated by Figs. 1(a) and 1(b). In addition, the conservation law of momentum requires that their transverse momentum vectors should satisfy $\mathbf{p}_A + \mathbf{p}_B = \mathbf{p}_P$, where the subscript P refers to the pump photon. Consequently, the radial components of their transverse momenta should be anticorrelated, i.e., $p_A^r = -p_B^r$, see Figs. 1(c) and 1(d), with the superscript r denoting the radial component. We can measure either the radial position correlation or radial momentum anticorrelation by varying the measurement settings. Strong correlations in both radial position and radial momentum are a key signature of entanglement. We thus approximate the EPR state by writing the two-photon wave function as

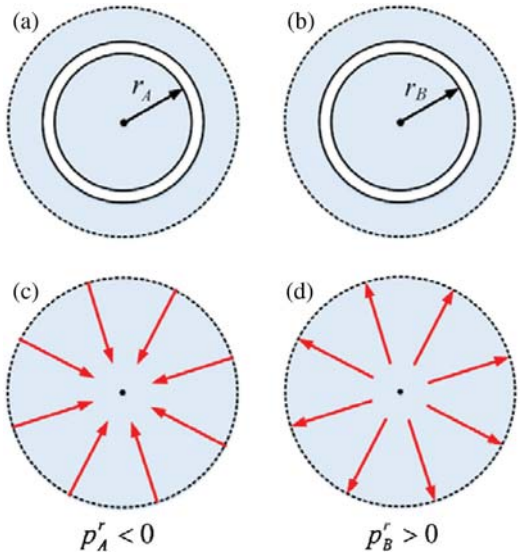

FIG. 1. Radial correlation of signal and idler photons in SPDC. (a) and (b) The radial positions are well correlated, $r_A = r_B$, while [(c) and (d)] the radial momenta are well anticorrelated, $p_A^r = -p_B^r$.

$$|\Psi\rangle_{AB} = \int |r\rangle_A |r\rangle_B dr = \int |p^r\rangle_A |-p^r\rangle_B dp^r, \quad (1)$$

In our experimental demonstration, the first key step is the formal definition and proper measurement of both the radial position and radial momentum variables of down-converted photons. The measurement of radial position is experimentally straightforward, which can be performed by defining a series of narrow radial slits in the form of annular apertures at different radii, see Fig. 1(a). This procedure is similar to that of using angular slits to measure the angular positions. However, the measurement of the radial momentum becomes, both conceptually and technically, more sophisticated. Before coming to this matter, we mention briefly the historical problem of the canonical definition of the radial momentum operator [38]. In cylindrical coordinates (r, ϕ, z), it can be naturally written as $\hat{P}_r = \mathbf{e}_r \cdot \hat{\mathbf{P}} = -i\hbar \mathbf{e}_r \cdot \nabla = -i\hbar \partial/\partial r$, where $\mathbf{e}_r$ is a unit vector along the radial axis. Subsequently, one can obtain directly its eigenstate, $\psi(r) \propto \exp(ik_r r)$, with $P_r = \hbar k_r$ being the eigenvalue. It seems that $\psi(r)$ has the correct form, because its appearance is highly similar to those of the linear momentum, $\exp(ip_x x/\hbar)$, and the angular momentum, $\exp(i\ell\phi)$. Unfortunately, such a definition has a critical issue that $\hat{P}_r$ is not really a Hermitian operator [39], since it is not equal to its adjoint, $\hat{P}_r^+ = -i\hbar[(\partial/\partial r) + (1/r)]$. Generally, one should cast the radial momentum operator into a symmetric form,

$$\hat{p}^r = \frac{1}{2}(\hat{P}_r + \hat{P}_r^+) = -i\hbar\left(\frac{\partial}{\partial r} + \frac{1}{2r}\right), \quad (2)$$

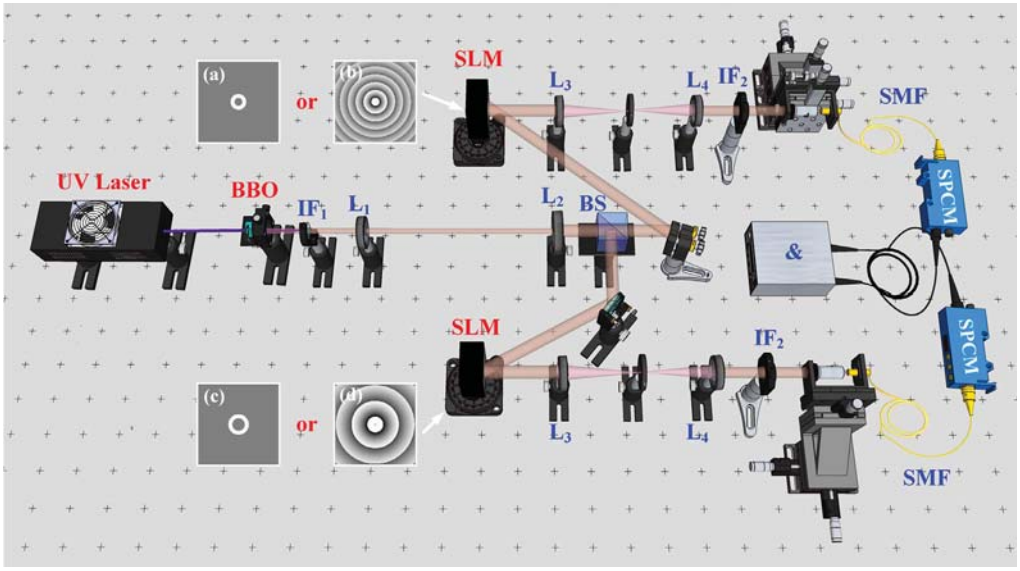

FIG. 2. Experimental setup (see the text for more details).

which is obviously Hermitian, i.e., $(\hat{p}^r)^+ = \hat{p}^r$. Dirac also stated in his textbook [40] on quantum mechanics that $\hat{p}^r$ is the "true momentum conjugate to r," which satisfies the fundamental commutation relation, $[r, \hat{p}^r] = i\hbar$. Thus, we are allowed to derive from Eq. (2) the radial momentum eigenstate as [41],

$$\psi_{p^r}(r) = \langle r|p^r\rangle = \frac{1}{2\pi\hbar}\frac{\exp(ip^r r/\hbar)}{\sqrt{r}}, \tag{3}$$

where p^r denotes the eigenvalue and it follows that $\hat{p}^r\langle r|p^r\rangle = p^r\langle r|p^r\rangle$. Here, based on Eq. (3), we use a projective measurement to determine the eigenvalues of radial momenta of both down-converted photons, which can be conveniently accomplished by the holographic method, e.g., using a computer-controlled spatial light modulator (SLM). The basic idea is to prepare a holographic grating with its phase front being conjugate to that described by Eq. (3). Thus either of the divergent $(p^r > 0)$ or convergent $(p^r < 0)$ wave front of the measured photons can then be made to be spatially flat $(p^r = 0)$ so that they can efficiently couple into a single-mode fiber by a collection lens.

Our experimental setup is sketched in Fig. 2, which is similar to that used for demonstrating the angular version of EPR correlations [25]. The SPDC is done by using a slightly focused beam from a mode-locked 355 nm ultraviolet laser to pump a 3-mm-thick BBO crystal to produce degenerate 710 nm down-converted photon pairs under the collinear type-I phase matching condition. A long-pass filter (IF_1) is used to block the pump beam after the crystal. The signal and idler photons are then separated by a nonpolarizing beam splitter (BS), and directed to illuminate independent SLMs. In each arm, we use two lenses of $f_1 = 200$ and $f_2 = 400$ mm to image the output facet of BBO crystal onto the SLM, and reimage the SLM onto the input facet of single-mode fiber (SMF) with another two lenses of $f_3 = 500$ and $f_4 = 2$ mm. Also, a 10 nm bandpass filter (IF_2) centered at 710 nm is placed in front of each SMF. The SMF is connected to a single photon counting module (SPCM), whose output is subsequently fed into a coincidence circuit with a time resolution of 25 ns. In our experiment, we prepare and display the desired holographic gratings with SLMs in both arms to measure the radial positions and radial momenta of signal and idler photons, respectively. The SLM (Hamamatsu, X13138-06) has a pixel array size of 1280×1024 with a pixel pitch of 12.5 μm. In a backward-propagation picture, the SLM together with SMF and SPCM just projects the incoming photons to the desired position or momentum states.

We prepare the radial slits, in the form of annular apertures with a narrow width, to define the radial positions, see the insets (a) and (c) in Fig. 2 for examples. Their transmission functions are mathematically described by a radial rectangle function, $\mathrm{rect}(r - r_{A,B}/\delta_{A,B})$, with $r_{A,B}$ denoting the central position of the radial slit and $\sigma_A = \sigma_B = 100$ μm (~8 pixels) being the radial width. In our experiment, we measure the two-dimensional joint probability distributions for the radial positions r_A and r_B. For each central position, r_A, of the radial slits placed in the signal arm, we scan the central positions, r_B, of the radial slits defined in the idler arm. After scanning r_A and r_B both in the range from 0.05 to 0.55 mm with an interval of $\Delta r = 12.5$ μm, we obtain the experimental results of the joint probability distribution as shown in Fig. 3(a). We observe a high joint probability distribution along the diagonal, which therefore indicates that the two-photon radial positions are well correlated. For easy visualization, we also plot the conditional probability $P(r_B|r_A)$ by scanning r_B when r_A is fixed at 0.20, 0.30, and 0.40 mm, respectively, see Figs. 3(b)–3(d). We then calculate the

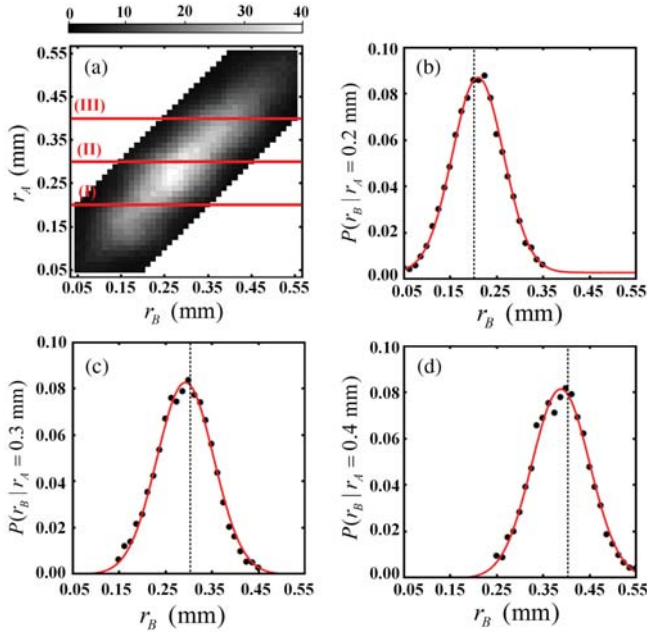

FIG. 3. Experimental results for radial position correlations. (a) Coincidence counts per second for r_A and r_B coordinates. (b), (c), and (d) The normalized probability corresponding to the lines across the regions in (a) where (I) $r_A = 0.2$, (II) 0.3, and (III) 0.4 mm, respectively. Dots are experimental data, red solid lines are Gaussian fits, and vertical dashed lines indicate the central radial positions of $r_B = 0.2$, 0.3, and 0.4 mm, respectively.

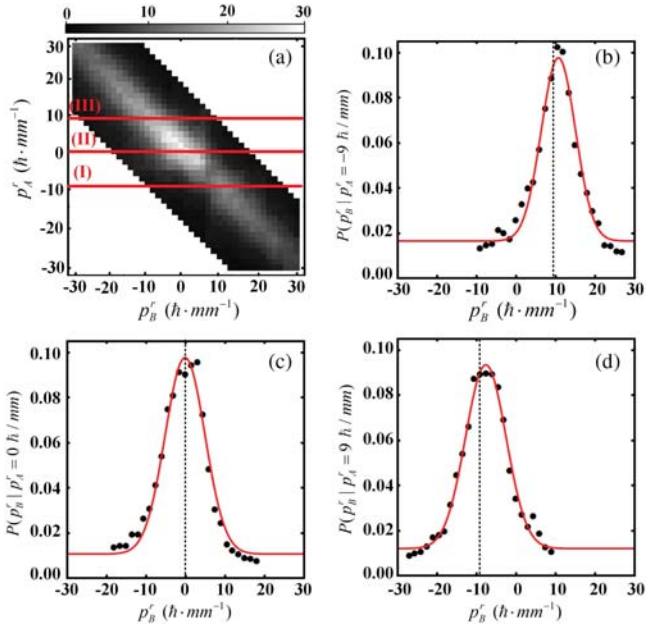

FIG. 4. Experimental results for radial momentum correlations. (a) Coincidence counts per second for p_A^r and p_B^r coordinates. (b), (c), and (d) The normalized probability curves corresponding to the lines across the regions in (a) where (I) $p_A^r = -9$, (II) 0, and (III) 9 $\hbar\,\mathrm{mm}^{-1}$, respectively. Dots are experimental data, red solid lines are Gaussian fits, and vertical dashed lines indicate the central radial momenta of $p_B^r = 9$, 0, and $-9\ \hbar\,\mathrm{mm}^{-1}$, respectively.

variance of the conditional probability according to the relation, $\Delta(r_B|r_A) = \sqrt{\int r_B^2 P(r_B|r_A)dr_B - (\int r_B P(r_B|r_A)dr_B)^2}$. Without any background subtraction, we obtain $\Delta(r_B|r_A = 0.2\ \mathrm{mm}) = 0.0574$, $\Delta(r_B|r_A = 0.3\ \mathrm{mm}) = 0.0584$, and $\Delta(r_B|r_A = 0.4\ \mathrm{mm}) = 0.0592$ mm. We thus find that $[\Delta(r_B|r_A)]^2 = (0.0034 \pm 0.00011)\ \mathrm{mm}^2$.

Next, in order to observe the radial momentum correlation, we prepare and display the desired holographic gratings on both SLMs to realize projective measurements of momentum eigenstates described by Eq. (3). We illustrate two typical gratings for such a purpose, as shown by the insets (b) and (d) in Fig. 2, which are both amplitude and phase modulated. Similarly, we measure a two-dimensional joint probability distribution for p_A^r and p_B^r coordinates, as presented in Fig. 4(a). Both p_A^r and p_B^r are scanned in the same range from -30 to 30 $\hbar\,\mathrm{mm}^{-1}$ with an interval of $\Delta p^r = 1.5\ \hbar\,\mathrm{mm}^{-1}$. Unlike positive position correlation, the antidiagonal feature of the joint distribution of Fig. 4(a) indicates that two-photon momenta are anticorrelated; i.e., high coincidence counts appear at the neighboring regions of $p_B^r = -p_A^r$. We also plot the conditional probability of $P(p_B^r|p_A^r)$ when the radial momentum eigenvalues of photon A are fixed at $p_A^r = -9$, 0, and 9 $\hbar\,\mathrm{mm}^{-1}$, respectively. In a similar way, we calculate the variance of the conditional probability according to the relation, $\Delta(p_B^r|p_A^r) = \sqrt{\int (p_B^r)^2 P(p_B^r|p_A^r)dp_B^r - (\int p_B^r P(p_B^r|p_A^r)dp_B^r)^2}$. Specifically, we obtain $\Delta(p_B^r|p_A^r = -9\hbar\mathrm{mm}^{-1}) = 7.565$, $\Delta(p_B^r|p_A^r = 0\ \hbar\,\mathrm{mm}^{-1}) = 7.041$, and $\Delta(p_B^r|p_A^r = 9\ \hbar\,\mathrm{mm}^{-1}) = 7.284$ $\hbar\,\mathrm{mm}^{-1}$ for Figs. 4(b), 4(c), and 4(d), respectively. As a result, we obtain $[\Delta(p_B^r|p_A^r)]^2 = (53.2872 \pm 3.8320)\hbar^2\mathrm{mm}^{-2}$.

In order to investigate the violation of the Heisenberg-like uncertainty principle, we now calculate the variance product and find that

$$[\Delta(r_B|r_A)]^2[\Delta(p_B^r|p_A^r)]^2 = (0.1814 \pm 0.0124)\ \hbar^2, \quad (4)$$

which is obviously smaller than the lower bound of 0.25 required by the EPR argument. If we further subtract the background to remove the accident counts, we obtain $[\Delta(r_B|r_A)]^2 = (0.0028 \pm 0.00017)\ \mathrm{mm}^2$ and $[\Delta(p_B^r|p_A^r)]^2 = (42.05 \pm 3.61)\ \hbar^2\,\mathrm{mm}^{-2}$, giving a variance product of $(0.1196 \pm 0.0110)\ \hbar^2$, approximately only half of the lower bound required by the EPR argument, hence showing an evident demonstration of EPR correlations.

In conclusion, we have demonstrated EPR correlations, for the first time, using radial degrees freedom of radial position and radial momentum of two down-converted photons. In the experiment, we use radial slits to define the radial positions and exploit the eigenmode projection to measure the radial momentum. The measured results for radial position correlation and radial momentum anti-correlation are found to violate the Heisenberg-like uncertainty

principle for independent particles, thus manifesting the quantum entangled nature of the radial structure of two-photon wave functions. Different from the unbounded and continuous nature of linear variables [13] and the periodically bounded or discrete nature of angular variables [25], the radial position is defined in a semi-infinite half-space. The use of radial properties offers several attractive features when compared to the scenarios using linear position and linear momentum or using angular position and angular momentum. First, unlike the analogous form of the linear momentum eigenstates to the OAM eigenstates, the canonical definition of radial momentum eigenstates is not straightforward but more sophisticated. In this regard, our work could shed light on the historical problem on the proper form of radial momentum operator. Second, our work suggests that each photon within a light beam of a complex amplitude described by Eq. (3) can carry a radial momentum of p^r. This suggestion may trigger some new experiments to use the additional radial d.o.f. of light beams to manipulate microscopic particles in optical tweezers. Third, as is well known, angular position and OAM are a conjugate pair of angular variables that have been extensively explored for quantum information science and technology. Our present work suggests that, in parallel with the angular position and OAM, the radial position and radial momentum can potentially offer a new platform for fundamental test of quantum mechanics and for novel application of quantum information.

L. C. thanks the support of the National Natural Science Foundation of China (91636109), the Fundamental Research Funds for the Central Universities at Xiamen University (20720190057), the Natural Science Foundation of Fujian Province of China for Distinguished Young Scientists (2015J06002), and the program for New Century Excellent Talents in University of China (NCET-13-0495). R. W. B. is thankful for the support by the Canada First Research Excellence Fund award on Transformative Quantum Technologies and by the Natural Sciences and Engineering Council of Canada (NSERC).

*chenlx@xmu.edu.cn

[1] R. Horodecki, P. Horodecki, M. Horodecki, and K. Horodecki, Quantum entanglement, Rev. Mod. Phys. **81**, 865 (2009).
[2] A. Einstein, B. Podolsky, and N. Rosen, Can quantum-mechanical description of physical reality be considered complete?, Phys. Rev. **47**, 777 (1935).
[3] *Quantum Theory*, edited by D. Bohm (Courier Corporation, North Chelmsford, 2012).
[4] J. S. Bell, On the Einstein-Podolsky-Rosen paradox, Physics **1**, 195 (1964).
[5] S. J. Freedman and J. F. Clauser, Experimental Test of Local Hidden-Variable Theories, Phys. Rev. Lett. **28**, 938 (1972).
[6] A. Aspect, P. Grangier, and G. Roger, Experimental Realization of Einstein-Podolsky-Rosen-Bohm Gedanken experiment: A New Violation of Bell's Inequalities, Phys. Rev. Lett. **49**, 91 (1982).
[7] D. Collins, N. Gisin, N. Linden, S. Massar, and S. Popescu, Bell Inequalities for Arbitrarily High-Dimensional Systems, Phys. Rev. Lett. **88**, 040404 (2002).
[8] A. Vaziri, G. Weihs, and A. Zeilinger, Experimental Two-Photon, Three-Dimensional Entanglement for Quantum Communication, Phys. Rev. Lett. **89**, 240401 (2002).
[9] A. C. Dada, J. Leach, G. S. Buller, M. J. Padgett, and E. Andersson, Experimental high-dimensional two-photon entanglement and violations of generalized Bell inequalities, Nat. Phys. **7**, 677 (2011).
[10] M. D. Reid, P. D. Drummond, W. P. Bowen, E. G. Cavalcanti, P. K. Lam, H. A. Bachor, U. L. Andersen, and G. Leuchs, Colloquium: The Einstein-Podolsky-Rosen paradox: From concepts to applications, Rev. Mod. Phys. **81**, 1727 (2009).
[11] M. D. Reid and P. D. Drummond, Quantum Correlations of Phase in Nondegenerate Parametric Oscillation, Phys. Rev. Lett. **60**, 2731 (1988).
[12] Z. Y. Ou, S. F. Pereira, H. J. Kimble, and K. C. Peng, Realization of the Einstein-Podolsky-Rosen Paradox for Continuous Variables, Phys. Rev. Lett. **68**, 3663 (1992).
[13] J. C. Howell, R. S. Bennink, S. J. Bentley, and R. W. Boyd, Realization of the Einstein-Podolsky-Rosen Paradox using Momentum- and Position-Entangled Photons from Spontaneous Parametric Down Conversion, Phys. Rev. Lett. **92**, 210403 (2004).
[14] K. Wagner, J. Janousek, V. Delaubert, H. Zou, C. Harb, N. Treps, J. F. Morizur, P. K. Lam, and H. A. Bachor, Entangling the spatial properties of laser beams, Science **321**, 541 (2008).
[15] V. Boyer, A. M. Marino, R. C. Pooser, and P. D. Lett, Entangled images from four-wave mixing, Science **321**, 544 (2008).
[16] M. P. Edgar, D. S. Tasca, F. Izdebski, R. E. Warburton, J. Leach, M. Agnew, G. S. Buller, R. W. Boyd, and M. J. Padgett, Imaging high-dimensional spatial entanglement with a camera, Nat. Commun. **3**, 984 (2012).
[17] P. Moreau, F. Devaux, and E. Lantz, Einstein-Podolsky-Rosen Paradox in Twin Images, Phys. Rev. Lett. **113**, 160401 (2014).
[18] H. Rubinsztein-Dunlop *et al.*, Roadmap on structured light, J. Opt. **19**, 013001 (2017).
[19] G. Molina-Terriza, J. P. Torres, and L. Torner, Twisted photons, Nat. Phys. **3**, 305 (2007).
[20] A. M. Yao and M. J. Padgett, Orbital angular momentum: Origins, behavior and applications, Adv. Opt. Photonics **3**, 161 (2011).
[21] M. Erhard, R. Fickler, M. Krenn, and A. Zeilinger, Twisted photons: New quantum perspectives in high dimensions, Light Sci. Appl. **7**, 17146 (2018).
[22] L. Allen, M. W. Beijersbergen, R. J. C. Spreeuw, and J. P. Woerdman, Orbital angular momentum of light and the transformation of Laguerre-Gaussian laser modes, Phys. Rev. A **45**, 8185 (1992).
[23] E. Yao, S. Franke-Arnold, J. Courtial, S. Barnett, and M. Padgett, Fourier relationship between angular position and optical orbital angular momentum, Opt. Express **14**, 9071 (2006).

[24] A. Mair, A. Vaziri, G. Weihs, and A. Zeilinger, Entanglement of the orbital angular momentum states of photons, Nature (London) **412**, 313 (2001).

[25] J. Leach, B. Jack, J. Romero, A. K. Jha, A. M. Yao, S. Franke-Arnold, D. G. Ireland, R. W. Boyd, S. M. Barnett, and M. J. Padgett, Quantum correlations in optical angle orbital angular momentum variables, Science **329**, 662 (2010).

[26] E. Karimi and E. Santamato, Radial coherent and intelligent states of paraxial wave equation, Opt. Lett. **37**, 2484 (2012).

[27] W. N. Plick and M. Krenn, Physical meaning of the radial index of Laguerre-Gauss beams, Phys. Rev. A **92**, 063841 (2015).

[28] E. Karimi, R. W. Boyd, P. de la Hoz,H. de Guise J. RehacekZ. Hradil, A. Aiello, G. Leuchs, and L. L. Sánchez-Soto, Radial quantum number of Laguerre-Gauss modes, Phys. Rev. A **89**, 063813 (2014).

[29] E. Karimi, D. Giovannini, E. Bolduc, N. Bent, F. M. Miatto, M. J. Padgett, and R. W. Boyd, Exploring the quantum nature of the radial degree of freedom of a photon via Hong-Ou-Mandel interference, Phys. Rev. A **89**, 013829 (2014).

[30] D. Zhang, X. Qiu, W. Zhang, and L. Chen, Violation of a Bell inequality in two-dimensional state-spaces for radial quantum number, Phys. Rev. A **98**, 042134 (2018).

[31] J. Leach, M. J. Padgett, S. M. Barnett, S. Franke-Arnold, and J. Courtial, Measuring the Orbital Angular Momentum of a Single Photon, Phys. Rev. Lett. **88**, 257901 (2002).

[32] G. C. Berkhout, M. P. Lavery, J. Courtial, M. W. Beijersbergen, and M. J. Padgett, Efficient Sorting of Orbital Angular Momentum States of Light, Phys. Rev. Lett. **105**, 153601 (2010).

[33] Y. Zhou, M. Mirhosseini, D. Fu, J. Zhao, S. M. H. Rafsanjani, A. E. Willner, and R. W. Boyd, Sorting Photons by Radial Quantum Number, Phys. Rev. Lett. **119**, 263602 (2017).

[34] X. Gu, M. Krenn, M. Erhard, and A. Zeilinger, Gouy Phase Radial Mode Sorter for Light: Concepts and Experiments, Phys. Rev. Lett. **120**, 103601 (2018).

[35] D. Fu, Y. Zhou, R. Qi, S. Oliver, Y. Wang, S. M. H. Rafsanjani, J. Zhao, M. Mirhosseini, Z. Shi, P. Zhang, and R. W. Boyd, Realization of a scalable Laguerre-Gaussian mode sorter based on a robust radial mode sorter, Opt. Express **26**, 33057 (2018).

[36] A. Trichili, C. Rosales-Guzmán, A. Dudley, B. Ndagano, A. B. Salem, M. Zghal, and A. Forbes, Optical communication beyond orbital angular momentum, Sci. Rep. **6**, 27674 (2016).

[37] K. Pang, C. Liu, G. Xie, Y. Ren, Z. Zhao, R. Zhang, Y. Cao, J. Zhao, H. Song, H. Song, L. Li, A. N. Willner, M. Tur, R. W. Boyd, and A. E. Willner, Demonstration of a 10 Mbit/s quantum communication link by encoding data on two Laguerre-Gaussian modes with different radial indices, Opt. Lett. **43**, 5639 (2018).

[38] R. L. Liboff, I. Nebenzahl, and H. H. Fleischmann, On the radial momentum operator, Am. J. Phys. **41**, 976 (1973).

[39] K. Fujikawa, Non-Hermitian radial momentum operator and path integrals in polar coordinates, Prog. Theor. Phys. **120**, 181 (2008).

[40] *The Principles of Quantum Mechanics*, 4th ed. edited by P. A. M. Dirac (Oxford University Press Oxford, 1995).

[41] J. Twamley, Quantum distribution functions for radial observables, J. Phys. A **31**, 4811 (1998).